Ad Hoc Networks 156 (2024) 103402

Contents lists available at ScienceDirect

Ad Hoc Networks

journal homepage: www.elsevier.com/locate/adhoc

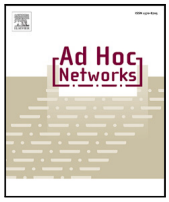

Link characteristics study of ultra-wideband radios

Alireza Ansaripour *, Milad Heydariaan, Omprakash Gnawali

University of Houston, Houston, TX, United States of America

ARTICLE INFO

Keywords:
Ultra-wideband
Physical layer
Wireless radio
Parameter selection
Link behavior

ABSTRACT

Comprehending the quality of links in diverse temporal and spatial environments is one of the critical steps in enhancing the performance of wireless applications. The increasing prevalence of ultra-wideband (UWB) radios in Internet of Things (IoT) applications for their precise ranging and localization capabilities, emphasizes the need to investigate the link quality (LQ) of UWB radios across different radio configurations, temporal settings, and spatial conditions. While previous observations studied the impact of these factors on LQ and its effect on communication, their practical applicability was limited and primarily focused on ranging and localization. Our first work in this study enhances the performance of previous adaptive-PHY layer algorithms by exploring and using intermediate radio configurations to enhance LQ. Additionally, we explore other LQ factors, previously studied in different wireless radios, in the context of UWB networks. The insights obtained from this study hold the potential to enhance the overall performance and efficiency of UWB applications.

1. Introduction

Indoor localization and ranging have become the cornerstone for many Internet of Things (IoT) applications. To address this need, the IEEE 802.15.4a standard and its later version, IEEE 802.15.4z, define a PHY layer called ultra-wideband (UWB), designed for precise localization and ranging. Major companies such as Apple, Samsung, NXP, and Decawave (now Qorvo) have integrated UWB radios into their products for applications related to localization and ranging. In addition to these primary use cases, researchers have also suggested using these radios for data communication among nodes in the network [1,2]. With this trend, the number of UWB-equipped devices will increase dramatically. As the number of UWB devices and applications grows, the need for high-performance protocols emerges to manage the network efficiently.

The quality of communication in wireless links is one of the essential performance factors in IoT applications, as it determines the probability of packet reception. Environmental factors create temporal and spatial dynamics that affect the quality of communication links. Researchers have developed real-world testbeds to study the impact of these factors on link quality (LQ) in different wireless technologies [3–6]. These studies have also provided guidelines to enhance LQ in the network to improve performance. A common approach to improve LQ is to modify the radio configuration. Adaptive PHY-layer approaches dynamically adjust the radio configuration to maximize performance based on the LQ of the links and the transmission cost of the packets.

With more than 25 000 different radio configurations, UWB radios provide a wide range of LQs and transmission costs for IoT applications to improve performance. Researchers have studied the impact of each PHY-layer parameter on link quality [7,8]. UWB chip manufacturers have also provided guidelines on radio configuration for different types of localization and data communication applications [9,10]. Although these studies were helpful on a preliminary basis, indicating the importance of understanding UWB communication and link quality, they need to be more comprehensive for most real-world implementations. These evaluations partially explored the UWB configuration space, offering limited radio configurations with low transmission cost or high LQ. However, using these radio configurations for an adaptive PHY-layer approach in UWB radio often results in sacrificing either LQ or other performance factors. Therefore, the research literature on UWB link quality has not yet been adequately explored compared to other radios, or they are not publicly available to researchers.

The study of temporal and spatial dynamics on UWB links has also been mainly limited to the ranging and localization capability of UWB radio in different line of sight (LOS) and non-line of sight (NLOS) conditions. Despite the importance of this topic, these studies are limited in exploring other crucial link characteristics that play a significant role in determining application performance, such as link symmetry and link quality fluctuation, which are essential for wireless applications.

To fill this gap, we conducted extensive experiments to observe the link quality of UWB radios. The first group of our experiments evaluated the impact of different UWB PHY-layer parameters on the

* Corresponding author.
E-mail address: alireza@cs.uh.edu (A. Ansaripour).

https://doi.org/10.1016/j.adhoc.2024.103402
Received 9 July 2022; Received in revised form 18 December 2023; Accepted 8 January 2024
Available online 18 January 2024
1570-8705/Published by Elsevier B.V.

LQ of UWB radios. Compared to previous studies [7–10], these experiments explored a wider range of radio configurations, observing LQ changes in different radio configurations. Instead of adopting the specific radio configuration with the highest LQ, our proposed method suggests an iterative config selection approach that finds the desired LQ while reducing overall performance loss. In the second group of our experiments, we derived inspiration from previous studies on LQ [3–6] and conducted extensive research on link behavior in UWB networks. We measured different temporal and spatial conditions to study LQ distribution, link symmetry, and LQ stability in UWB radio networks. Our experiments were conducted in various environments, using the previous UWB standard (IEEE802.15.4a) and the latest (IEEE802.15.4z). Our contributions are as follows:

- Experimental study of the effect of the UWB radio configuration on LQ.
- Experimental study of the behavior of UWB links across time and space.
- Designing an iterative config selection algorithm for improving LQ while enhancing application performance.

2. Related work

The network community generally defines LQ as the ratio of received packets. Based on LQ, they divided links into three major regions [4,6,11]. The good quality links are those with an LQ of more than 0.9. Links with $LQ < 0.1$ are considered bad quality links. The rest of the links are intermediate quality links. We followed these guidelines for our study.

Since radio signals travel through space, the dynamicity of the environment impacts LQ. Understanding the behavior of the link under these changes improves the performance of the network when designing wireless applications or MAC protocols [3,4]. The Roofnet project was an effort to improve the performance of the IEEE 802.11 mesh network designed to provide campus-wide internet connection [3].

Researchers have also conducted empirical experiments on IEEE 802.15.4 radio, validating some of the design principles such as link stability and link asymmetry used in designing wireless protocols for this radio technology [5,6]. Both these works emphasized the importance of understanding link behavior in the performance of the network application.

To improve the network's performance, some wireless technologies allow applications to change the radio configuration by modifying PHY-layer parameters. In such technologies, different configurations exhibit varying degrees of robustness against environmental factors like noise, attenuation, and interference. Configurations with lower robustness typically offer higher data rates, lower transmission power, and shorter transmission times, resulting in optimal performance when LQ is good. These configurations are also more susceptible to packet losses or corruption in wireless links. Configurations with higher robustness generally increase energy consumption and transmission time. However, when wireless links suffer from frame drops and retransmissions, switching to these configurations can improve the performance by reducing the ratio of packet drops.

Several studies have actively suggested dynamic adjustment of the radio configuration to maximize network performance under varying conditions. Related research in IEEE 802.11 proposed solutions modifying data rate [12–14] or transmission power [15] to optimize network performance in response to changes in LQ. Studying the impact of radio configurations on LQ becomes crucial when wireless technologies have numerous PHY-layer parameters. The exhaustive exploration of all possible configurations within a reasonable time frame is infeasible due to the vast configuration space. Studies have assessed the LQ for 1152 radio configurations in LoRa radios [16]. A similar investigation in the context of visible light communication (VLC) examined the LQ of 6480 different configurations to evaluate the effect of each parameter on link quality [17]. In these works, researchers provided guidelines on the impact of each radio parameter on LQ, narrowing down the search space for finding the desired radio configuration within the application context.

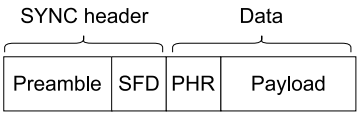

Fig. 1. UWB frame structure.

The existing literature on UWB LQ studies has utilized Channel Impulse Response (CIR) to estimate the propagation of the signal in space. Studies commonly used CIR to detect non-line-of-sight signal propagation, which impacts the performance of ranging and localization [18,19]. In addition to NLOS detection and mitigation, researchers have also discussed UWB link reliability in the presence of spatial factors such as constructive or destructive reflections of the signal [8] or interference from WiFi 6E, operating on the same center frequency as Channel 5 [7]. The research community has also provided guidance on configuring the radio to enhance application performance. Decawave suggests 16 different radio configurations for its UWB radio chip (DW1000), depending on the wireless application and communication range [9]. The DW1000 user manual [10] provides recommendations on selecting PHY layer parameters to improve link quality. Researchers have also conducted measurements to analyze the impact of individual PHY layer parameters on link quality in both previous and latest UWB standards [7,8].

In this study, our first goal is to improve the configuration selection in UWB links. Instead of suggesting only a limited number of radio configurations and abrupt changes to the PHY layer parameters, our approach dynamically adjusts the UWB PHY layer parameters based on the header and payload reception ratio. Our recommendations guide UWB applications through configuration space, allowing them to achieve the desired LQ while maintaining higher performance than robust configurations. Secondly, we conducted an extensive study on the link characteristics of UWB radio, similar to previous studies conducted in the context of IEEE802.15.4 [5,6]. Our findings on UWB link characteristics offer new insights not previously discussed in existing UWB studies [7,8,18]. These observations are highly relevant and beneficial for UWB applications, particularly in the areas of ranging, localization, and data communication. To ensure the generalizability of our conclusions, we developed testbeds in multiple environments. Furthermore, we varied the number and placement of nodes in different testbed configurations, enhancing the scalability and applicability of our observations across various dimensions.

3. Background

3.1. UWB frame structure

Based on the Decawave documentation [10] and the standard [20], the UWB frame consists of multiple parts, as shown in Fig. 1. The synchronization header, which includes the preamble and the start of the frame delimiter (SFD), detects the frame and synchronizes the sender and receiver. The data portion of the UWB frame contains the payload and the physical header (PHR).

3.2. Frame reception process in UWB radios

Fig. 2 presents the packet reception process flow chart in a UWB receiver. The receiver must first detect the preamble for successful packet delivery and synchronize with incoming symbols. If the receiver fails to detect the preamble, packet reception will fail, resulting in an LQ reduction. In some applications, if the receiver does not detect any

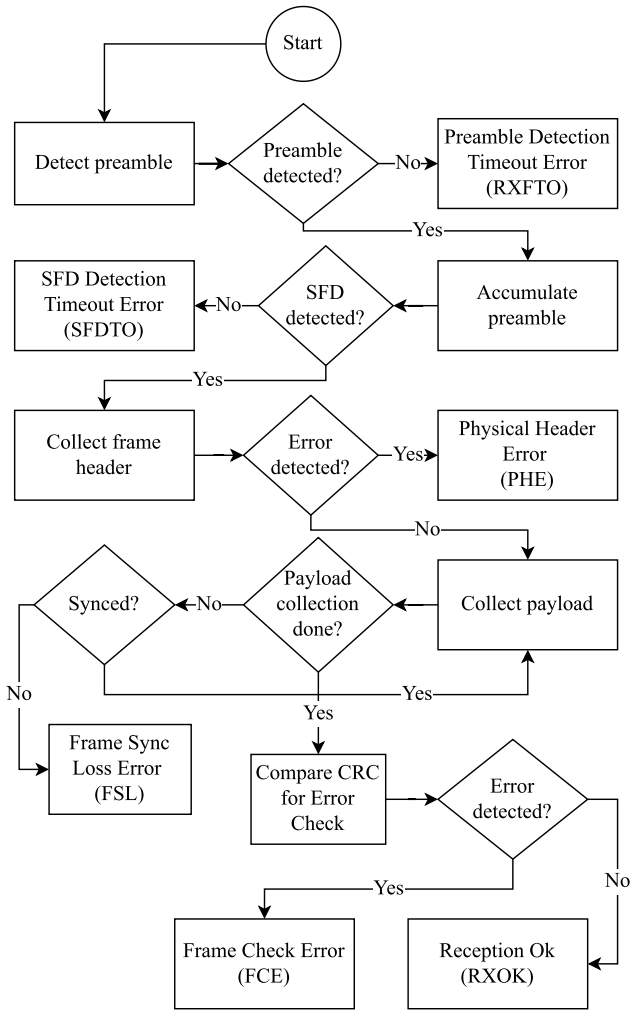

Fig. 2. UWB frame reception flow chart.

preamble after a time, the radio returns a frame detection timeout (RXFTO) error. Once synchronized, the receiver searches for the start of the frame delimiter (SFD) while accumulating preamble symbols. If the receiver fails to detect the SFD after spending a specific time collecting preamble symbols, it generates an SFD detection timeout (SFDTO) and terminates the reception with an error. Following the SFD, the receiver captures the physical header (PHR) and the payload, both of which are equipped with error check bits. If the checksum at the end of the PHR does not match its content, the radio raises a Physical Header Error (PHE). The receiver might also lose synchronization while collecting payload symbols, leading to a Frame Sync Loss (FSL) error. The packet reception is successful if the two-byte Cyclic Redundancy Check (CRC) at the end of the payload matches the data. If there is a mismatch, the receiver triggers the Frame Check Error (FCE).

3.3. UWB radio configuration

The IEEE 802.15.4a standard defines different parameters to configure the radio and modulate UWB frames. Table 1 overviews these parameters and their role in UWB frame modulation. The channel determines the center frequency and bandwidth of the modulation, impacting both the SYNC header and the data part of the UWB frame modulation. Pulse Repetition Frequency (PRF) determines the number of pulses used for each symbol in the frame modulation, determining the modulation of the entire frame. Preamble length (PLEN) defines the number of symbols in the preamble, and Preamble Code (PC) defines the combination of pulses in the preamble. Lastly, the data rate modifies the modulation of the payload section by indicating the mapping of data bits to symbols.

Table 1
UWB radio parameters and their impact on the modulation of the frame. The check marks indicate the parts of the frame that are impacted by each parameter.

Parameter name	SYNC header	Data
Channel	✓	✓
Preamble length (PLEN)	✓	
Preamble code (PC)	✓	
Pulse repetition Frequency (PRF)	✓	✓
Data rate (DR)		✓

Table 2
Testbeds used in UWB radio parameter evaluation.

Testbed name	Board	UWB radio chip	Environment type	Number of nodes
Hallway	Radino-L4	DW1000	Indoor	6
Bridge	Radino-L4	DW1000	Outdoor	6
CLOVES [21]	EVB1000	DW1000	Indoor	12
Office	EVB3000	DW3000	Indoor	9

4. Experiment design

We evaluated the link quality of UWB radios in various testbeds using multiple radio chips. Table 2 provides an enumeration of the testbeds, including the radio devices used and the environmental characteristics of each testbed.

4.1. Platform/Implementation

The Radino-L4 [22] and EVB1000 [23] boards utilize Decawave DW1000 chips for UWB communication. These radio chips are one of the successful implementations of the IEEE 802.15.4a standard that are widely used in UWB-based applications. Decawave is also a member of the FiRa consortium, which focuses on designing and developing UWB applications for localization and ranging. Several industrial products, including Pozyx, Radino, Uniset Sequitur, and Chiolas, have utilized the DW1000 chip to implement their RTLS systems. The office testbed used the DW3000 radio chip, which implements IEEE 802.15.4z for UWB radios. The EVB1000 and Radino-L4 boards have the same external antenna, while the EVB3000 utilizes a ceramic antenna mounted on the DWM3000 module. It is worth noting that the DW1000 chip has a smart transmission ability that allows for an additional power boost for frames with low transmission time, which is not defined in the standard. However, this feature was disabled in our study to ensure that the radio chip does not modify the configuration provided by the server.

4.2. Experiment environments and testbeds

The hallway testbed environment used in this study is similar to the one previously employed in UWB adaptive PHY layer research [8]. Fig. 3 illustrates the node placement for this environment. Node #0 is the transmitter, and the other five nodes are receivers. We repeated the experiment with the same node placement in the bridge testbed, which is an open space with one long side obstructed. Fig. 4 displays the experiment setting for this environment.

In the CLOVES testbed, we also increased the number of UWB nodes and links in addition to changing the environment. Fig. 5 displays the node placement in this testbed, along with the corresponding node IDs. Additionally, we created the office testbed to evaluate our results using the latest UWB standard (IEEE802.15.4z). Fig. 6 shows the node placement for this testbed. Both testbeds were deployed in

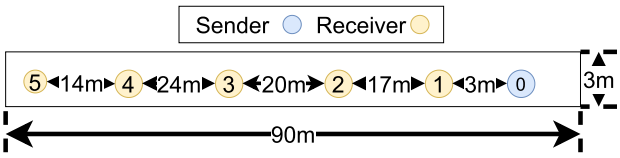

Fig. 3. Environmental settings for the hallway testbed.

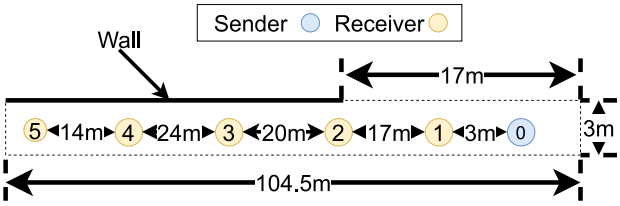

Fig. 4. Environmental settings for the bridge testbed.

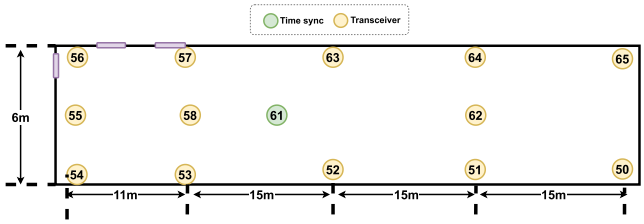

Fig. 5. Environmental settings for the CLOVES testbed.

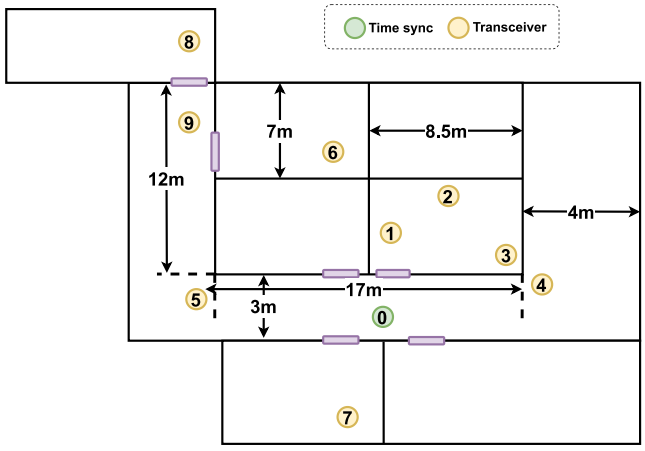

Fig. 6. Environmental settings for the office testbed.

environments coexisting with other radio technologies such as WiFi or Bluetooth.

To measure the amount of reflections and the NLOS of the received signals, we incorporated a method used for NLOS detection [24]. In this method, we first computed the received signal power level (RSL) and the first-path signal power level (FPSL) using diagnostic information provided by the radio chip upon frame reception and the formulas in the DW1000 user manual [10]. The difference between these two values ($RSL - FPSL$) indicates the amount of reflections during frame reception. If this value exceeds a threshold of 6 dB, this method suggests that the receiver did not capture the direct signal path and synchronized with one of the reflections. In this study, we used the $RSL - FPSL$ values from the radio in all testbeds to quantify the amount of reflections for each received packet.

Fig. 7 illustrates the cumulative distribution functions (CDFs) of the $RSL - FPSL$ values for the received packets in each testbed. The

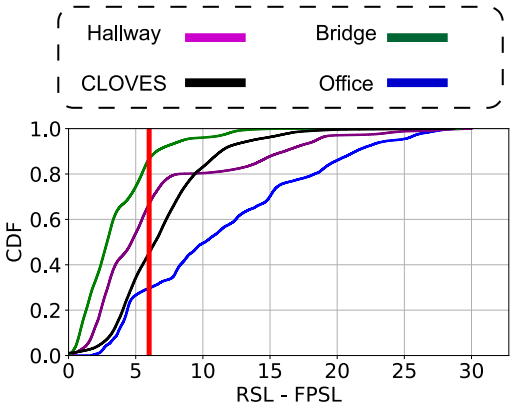

Fig. 7. Distribution of RSL-FPSL for all packets across different testbeds, with 6 dB as the indicator for LOS/NLOS signal. Links in the bridge, hallway, and CLOVES testbeds have mostly LOS connections, while links in the office testbed covered a wide range of reflections, highlighting the generalizability of the results.

bridge testbed, characterized by an open space environment, exhibited the lowest amount of reflections in the signals. As we transitioned to the hallway testbed, deployed in an indoor setting with similar conditions, the portion of reflections increased. In the CLOVES testbed, where signals were not obstructed by walls but influenced by the node placement, nearly half of the frames showed synchronization with one of the reflections. Lastly, in the office testbed, where we placed the nodes in different rooms, approximately 70% of the links experienced NLOS packet reception. Based on this, we can claim that the results of our study cover a wide range of signal propagations.

4.3. Experiment setups and radio configurations

Similar to previous works [7,8,10], our first experiment in the hallway and bridge testbed evaluated the impact of radio parameters on the quality of UWB links. Table 3 describes the UWB radio configuration parameters and their values. The IEEE 802.15.4a standard defines 24 preamble codes (PC) to create complex channels for simultaneous communication. However, the standard only recommends a few for each pair of channels and pulse repetition frequency. We chose one of the recommended PCs for the hallway and bridge experiments. For transmission power, we chose the values 0xA0A0A0A0 for low-power transmission and 0 × 0C0C0C0C for high-power transmission. Table 3 describes their equivalent dB values. We created a pool of 432 radio configurations using these parameters and measured the LQ in the hallway and the bridge testbeds.

We tested each radio configuration in intervals of 200 packets. In each interval, we first configured all nodes to one of the radio configurations. Once the configuration was successful on all nodes, node #0 started transmitting while others were logging the received packets. To ensure the correctness of data collection throughout the experiment, we designated a specific radio configuration known as the *indicator config*. The transmitter often (in our experiment, every ten intervals of transmission) switched to this configuration to ensure that the receivers were correctly receiving packets throughout the experiment.

In the office and CLOVES testbeds, the first group of our experiments validated the findings from the bridge and the hallway testbeds. In these testbeds, the timeSync node (node # 0 in the office and node # 61 in the CLOVES testbed) determined the start of each interval and broadcasted the radio configuration to all nodes. This node also selected the transmitter node for each interval. In each interval, the transmitter node transmits 100 packets while the remaining nodes record the received packets or reception errors. Table 4 lists all the experiments for the UWB PHY-layer study. Apart from the Channel

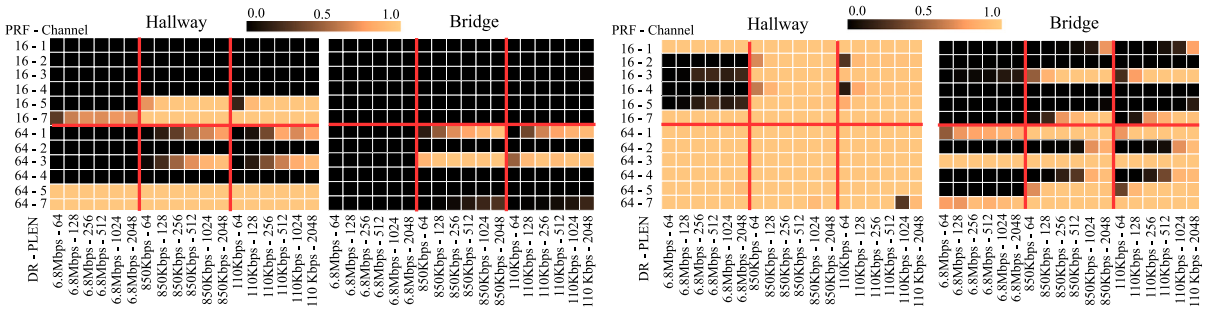

(a) LQ heatmap of Node 2 with 0xA0A0A0A0 power gain (low-power transmission)

(b) LQ heatmap of Node 5 with 0x0C0C0C0C power gain (high-power transmission)

Fig. 8. Link quality heatmap in the hallway and the bridge testbeds. The X-axis reflects data rate (DR) and preamble length (PLEN), and the Y-axis represents channel and pulse repetition frequency (PRF). Each cell displays the LQ corresponding to its configuration.

Table 3
Radio configuration parameters and their values used for bridge and hallway testbeds. In total, we evaluated 432 radio configurations in these two testbeds.

Parameter name	Values
Channel	1, 2, 3, 4, 5, 7
Preamble length (PLEN)	64, 128, 256 512, 1024, 2048
Pulse repetition frequency (PRF)	16, 64
Preamble code (PC)	R (recommended by standard [20])
Preamble Acquisition Chunk (PAC) size	R (recommended by standard [20])
Data rate (DR)	110 kbps, 850 kbps, 6.8 mbps
Transmission power gain	0xA0A0A0A0 (3.0 dB) 0x0C0C0C0C (24.0 dB)

Table 4
List of experiments in the office and the CLOVES testbeds.

Experiment name	Purpose of the experiment
PAC-PLEN	Selection of proper PAC and PLEN
PRF	Impact of changing PRF on SHR
Channel	Impact of changing UWB channel on SHR
PC	Impact of changing PC on SHR
SYNC	Impact of synchronization on PRR
Data rate	Impact of changing data rates on PRR

experiment, we used channel 5 for all other experiments as it is the only common channel between the DW1000 and DW3000 radio chips.

To investigate the impact of temporal and spatial factors on the quality of UWB links, we conducted extended experiments lasting 36 h in the CLOVES testbed and 26 h in the office testbed. The experiments were divided into two-hour data collection periods spanning four days from Tuesday to Friday, including working hours and weekends. We reduced the number of radio configurations to increase the number of repetitions and the number of transmitted frames per iteration. Within each iteration, the sender node sent 1000 frames over 60 s in the office testbed and 30 s in the CLOVES testbed. During each two hours, each node transmitted twice using each radio configuration.

5. Impact of UWB radio configuration on link quality

To understand the impact of UWB radio configuration on LQ, we first focused on the results of the hallway and the bridge testbed. Similar to other studies in link characteristics, we use packet reception ratio to estimate and compare LQ. To present our results, we chose Node #2 for low-power and Node #5 for high-power transmission and plotted the LQ heatmap of the configurations with the recommended PC in Fig. 8 for both environments. We used the data from the other nodes to support our hypothesis. The x-axis of the heatmap shows the values for PLEN and DR, and the y-axis represents the values for PRF and Channel.

Previous studies [8,10] have highlighted that UWB configurations in the top left corner of the heatmap (PLEN 64, DR 6.8 Mbps, PRF 16) offer higher performance by reducing energy consumption and transmission time of the frame. Conversely, configurations in the right column (PLEN 2048, DR 110 kbps, PRF 16) provide the highest robustness against environmental changes, resulting in superior LQ. Fig. 8 supports these findings by demonstrating that transitioning from high-performance to high-reliability configurations enhanced link quality without altering transmission power in some links.

Although high-reliability configurations provide the highest LQ, it is important to note that they require approximately 46 times more energy and 49 times more transmission time compared to high-performance configurations when frames use a 127-byte payload. Fig. 8 also demonstrates that, in most cases, there is an opportunity to enhance LQ while mitigating the trade-off between LQ and other performance metrics by adopting intermediate configurations. In the hallway testbed, when the sender utilized the high-performance radio configuration (DR 6.8 Mbps, PRF 16, PLEN 64) on channel 5, link $0 \rightarrow 2$ suffered from poor LQ. By changing the PRF from 16 to 64, this link reached the same LQ as the high-reliability configuration. However, this configuration change resulted in approximately a 5% increase in transmission time and an 11% increase in transmission power.

UWB applications can achieve satisfactory link quality by utilizing intermediate radio configurations without compromising overall performance. However, as illustrated in Fig. 8, the multitude of available configurations presents a challenge when selecting the optimal radio configuration. To address this issue, we develop a heuristic approach that reduces the exploration space to find the favorable LQ.

5.1. Improving SYNC header reception

While improving SYNC header reception may not directly enhance link quality, it plays a crucial role in the overall performance, as the number of received packets cannot surpass the number of detected SYNC headers. In UWB communication, environmental factors can corrupt preamble symbols, making them undetectable by the receiver. The UWB standard and Decawave radio chips allow applications to adjust the radio configuration to increase the SYNC header reception ratio (SHR).

5.1.1. Impact of preamble length and PAC size on SHR

In UWB receivers, SYNC header detection involves cross-correlating the incoming symbols with a window of preamble symbols, generating a channel input response (CIR). The CIR is then compared to an estimate. If similarity exceeds a predefined threshold, the receiver triggers the SYNC header detection signal. UWB receivers can enhance SHR by modifying the PAC (Preamble Acquisition Chunk) size in the radio configuration that determines the window size for the cross-correlation. By increasing the PAC size, the receiver increases the

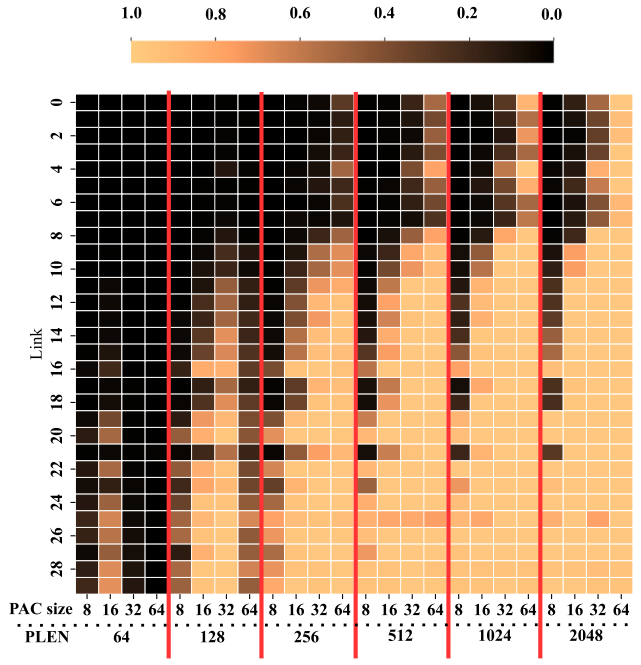

Fig. 9. SYNC header reception ratio (SHR) for UWB links in the CLOVES testbed with varying PAC size and PLEN. PAC size 64 demonstrates the highest enhancement in SHR when the sender used PLENs 256 and higher for frame transmission. To maximize SHR, the receiver should switch to PAC size 64, while the sender should begin with PLEN 256 and progressively increase it until achieving the desired SHR for the link.

chance of header reception by using more symbols in the preamble detection process [7,10].

For a successful preamble detection, the receiver must accumulate a minimum number of preamble symbols. We refer to this as the Minimum number of Accumulated Symbols (MAS). For example in the DW3000 radio chip, the MAS is 12 symbols greater than the PAC size. Thus, when receivers increase PAC size for higher SHR, senders also need to use proper PLENs, making sure receivers have sufficient symbols to accumulate. The DW1000 user manual recommends longer PLENs for larger PAC sizes.

The results of the hallway and bridge testbeds indicate that 71 radio configurations experienced more than 20% LQ improvement when switching to higher PLENs and using the recommended PAC size. However, the recommended PLENs in the DW1000 user manual [10] are significantly larger than MAS. To further optimize the matching between the PLEN and the PAC size, the PLEN-PAC experiment measured the SYNC header reception rate (SHR) of the receivers with different PLENs and PAC sizes. Fig. 9 illustrates the SHR for 29 links in the CLOVES with more than 20% improvement in SHR when transitioning from the lowest PLEN and PAC size to the highest. PAC 64 and 32 had the lowest SHR for PLEN 64. Due to the higher MAS and the potential loss of preamble symbols, PLEN 64 cannot provide sufficient preamble symbols for the receiver to detect the preamble. We also observed this trend for PLEN 128. However, starting from PLEN 256, PAC 64 consistently provided the highest SHR. We also obtained the same behavior with the DW3000 nodes in the office testbed when nodes used PAC 32 with PLEN 128. Based on the results of the PAC-PLEN experiment, Table 5 describes our mapping for DW1000 and DW3000.

Fig. 9 also states that switching to PLENs higher than 256 while using PAC 64 resulted higher SHR for nine nodes in the CLOVES testbed. Thus, to increase SHR, receiver sets the PAC size to a higher value and the sender sets the PLEN according to Table 5. Then, the sender iteratively increase the PLEN to achieve the desired SHR.

Table 5
Recommended PLEN for PAC sizes for DW1000 and DW3000. The PLEN - PAC size recommendation differs for each radio technology and the MAS. Our recommendation includes more symbols than MAS to tackle symbol corruptions occurring along the path of the signal.

DW1000			
PAC size	8	16	64
PLEN	64	128	256<
DW3000			
PAC size	16	32	32
PLEN	64	128	128<

Table 6
Supported UWB channels for each radio chip and the number of links with the highest SHR when switching to that channel. In contrast to previous works, there is no channel providing highest SHR and LQ for all UWB links.

Channel	1	2	3	4	5	7	9
CLOVES (DW1000)	5	0	0	2	0	25	–
Office (DW3000)	–	–	–	–	18	–	2

5.1.2. Impact of pulse repetition frequency (PRF) and preamble code (PC) on SHR

The pulse repetition frequency (PRF) is another parameter at the physical layer of UWB radio that determines the number of pulses per preamble and data symbol. Previous studies have recommended using PRF 16 due to lower power consumption [8,10]. However, increasing the PRF to 64 can enhance symbol robustness by using more pulses per symbol. This reduces symbol distortion, making it easier for the receiver to detect and accumulate preamble symbols, ultimately resulting in a higher SHR. Among 108 radio configurations in the hallway and the bridge testbeds that used PRF 16, 93 of them experienced higher LQ when switching to PRF 64. The PRF experiment evaluated the impact of PRF and PLEN on SHR in both the CLOVES and the office testbeds. For each PLEN, we selected PAC size according to Table 5. Table 7 compares the number of links with good SHR ($SHR > 0.9$) for both the office and the CLOVES testbeds when links switched from PRF 16 to PRF 64. The results indicate that increasing PRF enhanced SHR in all PLENs.

The results of the PC experiment, which involved two preamble codes for PRF 16 and PRF 64, revealed that less than 1% of the links in both the CLOVES and office testbeds experienced an SHR change of more than 20% when switching between preamble codes. This finding suggests that the PC does not significantly affect LQ since it only determines the sequence of the preamble symbols.

5.1.3. Impact of center frequency and bandwidth on SHR

Previous works have also acknowledged the importance of channel switching on LQ improvement [8,10]. These studies suggest switching to channels with lower center frequencies or higher bandwidths. However, the results obtained from our hallway and bridge testbeds partially contradict this finding. According to Fig. 8(a), although channel 7 had the highest center frequency among all UWB channels in DW1000, it provided the highest LQ for links in the hallway testbed. In our channel experiment in the office and the CLOVES testbed, we configured links with different channels and studied links that experienced more than 20% SHR improvement when switching channels. Table 6 illustrates the supported channels for each radio device along with the number of links having the highest SHR when switching to that channel. According to the results in the CLOVES testbed, when two channels had the same center frequency, the one with higher bandwidth provided higher SHR (e.g., channel 5 vs. 7 or 2 vs. 4). We also observed that channel 7 with the highest center frequency provided the highest LQ for 25 links in this testbed. In the office testbed, when switching between channels 5 and 9, 18 links had higher SHR with channel 5, which has a lower center frequency, and only two

Table 7
Number of links with $SHR > 0.9$ using different PLEN and PRF. Increasing both PLEN and PRF along with choosing the appropriate PAC size contributes to higher SHRs in UWB links.

	PLEN	64	128	256	512	1024	2048
CLOVES	PRF 16	21	50	59	63	66	71
	PRF 64	74	95	104	108	110	115
Office	PRF 16	25	25	26	22	27	32
	PRF 64	37	41	43	45	41	41

Table 8
Error distribution when using DR 6.8 Mbps. Approximately 99% of the reception errors occur during data reception, when the receiver is capturing the physical header or the payload.

	SYNC HDR	Data		
	SFDTO	PHE	FSL	FCE
ClOVES	0.2%	17.9%	79.1%	2.8%
Office	0.0%	62.7%	36.1%	1.2%

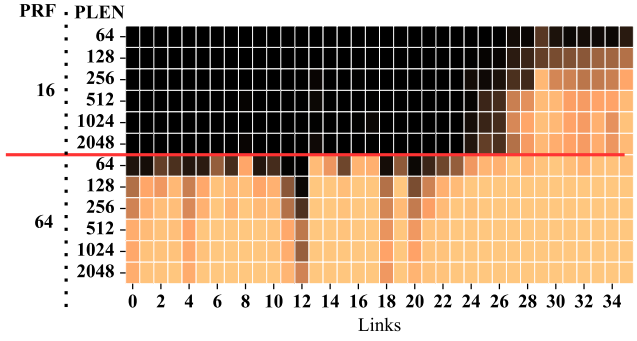

Fig. 10. Impact of using higher PLEN and PRF size on PRR of UWB frames. Out of 47 links with $SHR > 0.9$ and low PRR, 36 links gained more LQ when switching to configurations with higher PLEN and PRF.

links had higher SHR with channel 5. Based on the results, no channel provides the highest SHR in all UWB links. If the receiver and sender have multiple common channels, the application must switch between them to find the best channel, focusing on those with higher bandwidth.

5.2. Improving payload reception

After improving SHR, the next step is to improve the packet reception rate (PRR). Reception errors occurring after SYNC header detection cause reception fails, contributing to lower LQ. To analyze the gap between SHR and PRR, Table 8 demonstrates the distribution of each error type. Based on this table, the majority of these errors are Frame Sync Loss (FSL) and Physical Header Error (PHE) that occur during the reception of the payload. The goal of this section is to reduce these errors to increase PRR.

5.2.1. Impact of synchronization on PRR

In wireless networks, preambles also synchronize the receiver clock with the sender, which is crucial for extracting symbols from the incoming signal. As preamble symbols travel through the wireless channel, the receiver may miss some of them due to corruption. This reduces the quality of synchronization, leading to FSL or PHE.

To enhance synchronization quality, UWB nodes can increase the robustness of the preamble symbols by switching to higher PRFs or increasing the PLEN. This increase provides the receiver with more samples to synchronize. The results of the hallway and bridge testbeds demonstrated that increasing the PRF and PLEN resulted in higher LQs in certain configurations. In our SYNC experiment, 47 links had SHR greater than 0.9 while maintaining a PRR lower than 0.5 when using PLEN 128 in the CLOVES testbed. Fig. 10 illustrates 35 of these links that gained higher LQs when switching to higher PLENs or PRFs. We also observed that increasing PLEN does not always enhance synchronization. When links had $SHR < 0.9$ with $PLEN = 256$, increasing PLEN no longer helped synchronization quality and only contributed to higher reception errors. Thus, synchronization improvement works when the links have a good SHR with small PLENs.

5.2.2. Impact of data-rate on PRR

When increasing PLEN and PRF cannot provide sufficient synchronization quality, links need to reduce the data rate to increase the transmission time for each sample. By doing so, the receiver can extract bits from the symbols, even with less precise synchronization. The results of the hallway and the bridge testbed suggest that links can have up to 100% LQ improvement when switching from DR 6.8 Mbps to 850 kbps (e.g., Fig. 8(a) Channel 5 and PRF 16). Meanwhile, LQs were mostly similar when switching from DR 850 kbps to 110 kbps. In these links with low SHR, decreasing DR will not impact LQ due to a lack of preamble detection.

5.3. Analyzing the performance of radio configuration parameters

To understand the performance reduction/gain when changing radio configurations, this section discusses the impact of changing each parameter on energy consumption and transmission time. Eq. (1) calculates the energy and the time to send or receive a UWB frame. T_{SYNC} and P_{SYNC} represent the SYNC header's transmission time and energy consumption. T_{Data} and T_{Data} are the data portion's transmission time and power consumption.

$$\begin{aligned} E &= T_{SYNC} * P_{SYNC} + T_{Data} * P_{Data} \\ T &= T_{SYNC} + T_{Data} \end{aligned} \tag{1}$$

UWB nodes must increase PLEN, PAC size, and PRF for higher SHR. When switching from PRF 16 to 64, P_{SYNC} increases 24% while the other three parameters will be the same. In the UWB standard, each preamble symbol is approximately 1 μs. By increasing PLEN, the UWB sender increases T_{SYNC}, leading to higher transmission time and higher energy consumption. Increasing the PAC size does not impact the transmission time or energy consumption since it only determines the sample size for the preamble detection phase.

UWB radios can also switch from DR 6.8 Mbps to 850 kbps for highest data reception rate. According to the DW1000 data sheet [9], this change reduces P_{Data} by 20% but increases T_{Data} by 635%. Considering these two changes, energy consumption for payload modulation increases by approximately 588% when switching from 6.8 Mbps to 850 kbps. Similarly, when switching from DR 850 kbps to 110 kbps, P_{Data} decreases by 2%, but T_{Data} increases by 800%.

6. Iterative LQ improvement for UWB links

In this section, we develop a config change algorithm for UWB links that dynamically chooses the appropriate radio configuration that satisfies the LQ of the application. Instead of switching to the most robust configuration with the lowest performance, our design aims to enhance LQ while reducing performance loss.

Fig. 11 illustrates the flow of the config change algorithm. This algorithm first checks if the LQ of the link is lower than the desired threshold of the application (LQ_{thresh}). If higher LQ is required, our algorithm uses these three approaches: (1) SHR improvement, (2) SYNC improvement, (3) DR decrease. Initially, SHR improvement iteratively increases SHR until $SHR > LQ_{thresh}$. In the SHR improvement phase, the algorithm initially increases PRF since it has the lowest energy consumption and transmission time increase. If further SHR improvement is required, the algorithm increases PAC size and PLEN. Once the link has sufficient SHR, the algorithm stores the preamble length in PLEN*. In the payload reception improvement phase, the algorithm first tries

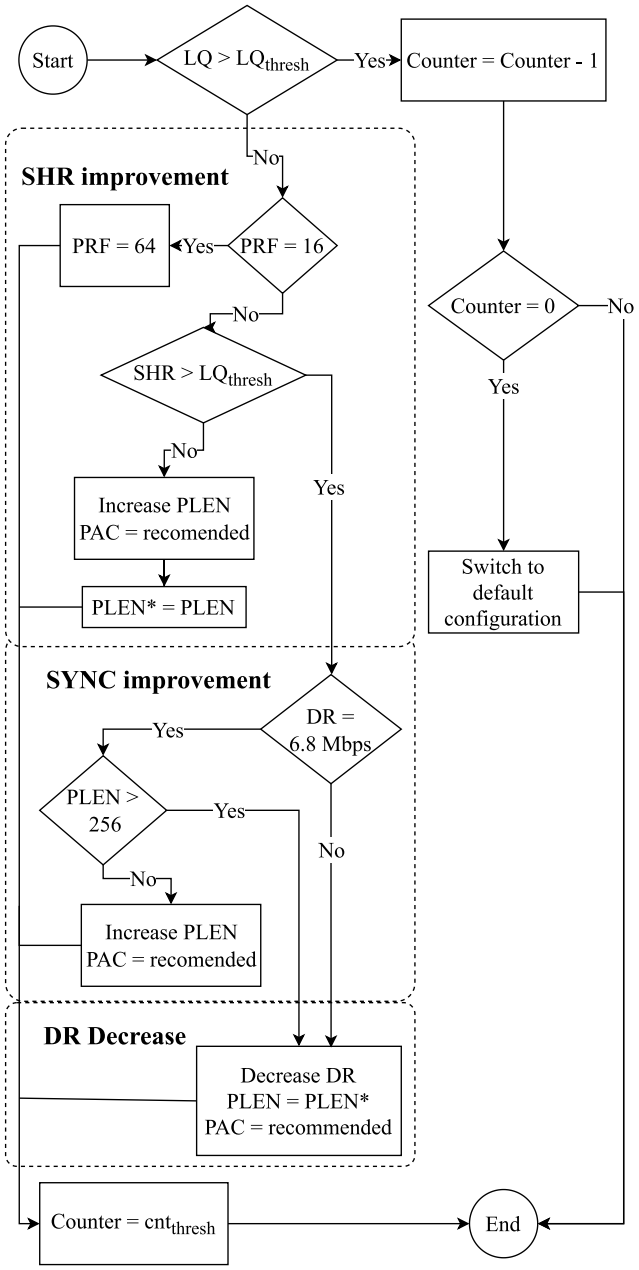

Fig. 11. Decision flow diagram for the config change algorithm. To increase LQ, the algorithm first tries to enhance SHR. The second step to improve LQ is enhancing synchronization. Finally, the algorithm reduces DR to decrease the error rate and improve LQ.

to improve synchronization by increasing the preamble length of the frames. For PLENs smaller than 256, reducing the data rate results in higher transmission time and energy consumption than increasing the PLEN. Finally, if synchronization improvement cannot provide satisfactory LQ, the algorithm sets the preamble length to PLEN* and starts reducing the data rate for LQ enhancement.

Although UWB radio chips provide diagnostic information to assess signal reception quality, our config change algorithm uses SHR, LQ and current radio configuration as input. One of the main challenges with using diagnostic information is its availability. In UWB chips, these parameters are only available when the receiver successfully captures the physical header. During SHR improvement, these parameters are mostly unavailable when the receiver is not detecting a large portion of the preambles. Considering these parameters for payload reception

Table 9
Energy consumption and transmission time for different UWB radio configuration. The first row is the default configuration providing the lowest transmission time and energy consumption and last row is known for providing highest robustness. Changing the PAC size has not impact on energy consumption since it only changes the number of PLEN symbols in the cross-correlation.

Config ID	PRF	PLEN	DR (kbps)	Transmission time (μs)	Energy (μJ)
0	16	64	6800	247.95	51.9
1	64	64	6800	259.68	57.6
2	64	256	6800	445.06	118.47
3	64	256	850	1529.17	300.0
4	64	512	850	1789.68	381.18
5	64	1024	850	2310.71	543.52
6	64	2048	850	3352.76	868.22

improvement does not change our algorithm's outcome. When the link is experiencing huge amounts of error, the radio chip can either increase PLEN for better synchronization or decrease the data rate. Based on our observations in Section 5.2, using SHR and the current configuration, the config change algorithm can decide whether to improve synchronization or reduce the data rate.

Table 9 illustrates the power consumption and transmission time for radio configurations used in this algorithm. The first row (config ID 0) describes the radio configuration with the lowest transmission time and power consumption and the last row (config ID 6) provides the highest robustness for UWB applications. In this table, we chose the maximum standard size payload of 127 bytes for our frames.

Since wireless networks operate in a dynamic environment, destructive factors can vanish or decrease over time. In such scenarios, applications can improve communication performance by reducing the cost of frame transmission. If $LQ > LQ_{thresh}$, the config change algorithm reverts to the default configuration to find a new radio configuration. To avoid frequent LQ changes caused by resetting the radio configuration, hysteresis can be used to smoothen the LQ. However, it is also critical for config change algorithm to adapt to short-term environmental changes. With the *counter* variable, the config change algorithm aims to rapidly achieve $LQ > LQ_{thresh}$ to minimize frame losses. Once the $LQ > LQ_{thresh}$, the algorithm checks the stability for a few rounds based on the counter's value. Once the counter reaches 0, our algorithm resets the radio configuration to check if a new radio configuration can satisfy $LQ > LQ_{thresh}$ while providing higher performance.

6.1. Performance evaluation of config change

To evaluate the effectiveness of our config change algorithm in terms of LQ, energy consumption, and transmission time, we conducted evaluations in both the office and the CLOVES testbeds. We set $LQ_{thres} = 0.9$ in our evaluation and compared our results with the DecaWave recommendation. Fig. 12 illustrates the results of our comparison in the CLOVES testbed. According to the figure, 10% of the links had good LQ with the high-performance radio configuration. Both the config change and the DW recommendation utilized this radio configuration since no further LQ improvement was required for these links. The DW recommendation switched to the high-robustness setting for the remaining links that demanded higher LQ. However, by utilizing intermediate configurations, the iterative config change approach mitigated this trade-off in 80 links within the CLOVES testbed, achieving 46% lower energy consumption and transmission time in this testbed. In the office testbed, 23% of the links demonstrated good LQ using the high-performance radio configuration. Both the DW recommendation and the config change approach increased this ratio to 51%. Our algorithm further reduced the transmission time and energy consumption for 22 links in the office testbed, reducing both energy consumption and transmission power by 32% in this testbed.

For UWB applications with energy constraints, we also considered a config change energy-constrained (EC) scenario, where config change

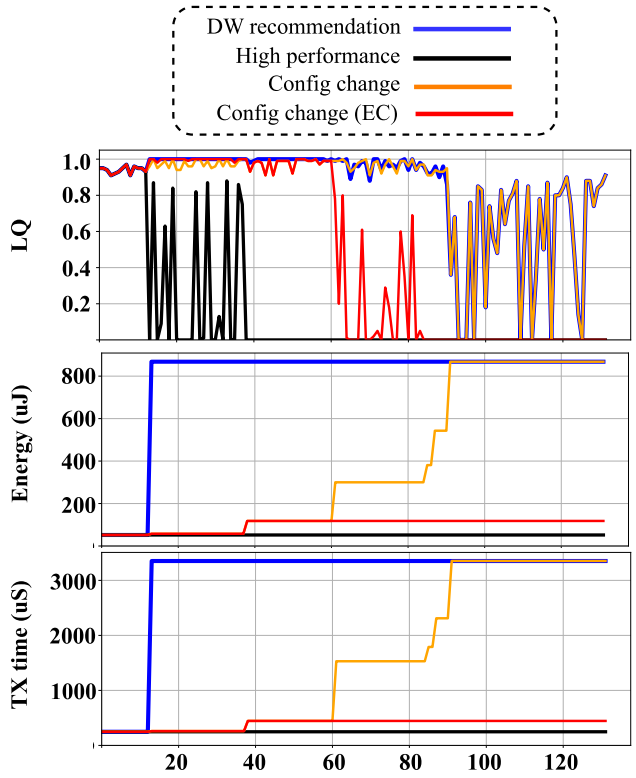

Fig. 12. Comparison of LQ, energy consumption, and transmission time (TX time) of frames using different approaches in the CLOVES testbed. Our proposed solution achieves an LQ similar to the DecaWave recommendation while demonstrating lower energy consumption and shorter transmission time in 60% of the links.

sets a threshold on energy consumption and does not exceed that value. In this evaluation, we limited our applications to only use 6.8 Mbps. According to Fig. 12, config change (EC) still outperforms the high-performance radio configuration while satisfying the energy constraint limitation. The config change (EC) provided better LQ in 30 links in the office and 56 links in the CLOVES testbeds.

6.2. Hysteresis analysis in config selection

In this section, we evaluate the impact of hysteresis in determining the LQ of the links. In our long-run experiment in the CLOVES testbed, we used different cnt_{thresh} for our config change algorithm and recorded the LQ of the links in each iteration. Fig. 13 shows the average LQ of the links using different cnt_{thresh}. Although choosing a low cnt_{thresh} makes the algorithm more adaptive to changes, links experienced 27% lower LQ with $cnt_{thresh} = 2$ compared to when $cnt_{thresh} = 14$.

To maintain the average LQ close to the best LQ of the link, applications have the option to adjust cnt_{thresh} individually for each link. As depicted in Fig. 13, the initial 17 links and the final 30 links had similar average LQ regardless of cnt_{thresh}. For these links, the application can select a low cnt_{thresh}. In situations where the default radio configuration consistently provides bad LQ, applications can also switch to an alternative radio configuration when cnt_{thresh} reaches zero.

7. Link characteristics study in UWB network

This section focuses on analyzing our long-run experiments, which aim to assess the behavior of UWB links in the face of environmental changes. Before our study, researchers conducted similar investigations for various radio technologies [3,5,6], emphasizing the significance of these studies in determining link performance. Here, we examine the same parameters evaluated in previous works to gain insights into the behavior of UWB radios in different environmental conditions.

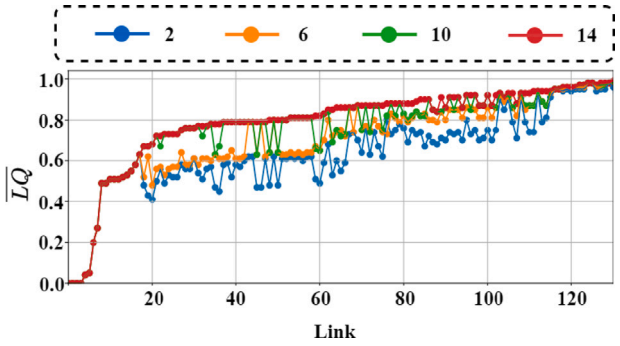

Fig. 13. The average LQ of the links ($\overline{LQ}$) in the CLOVES testbed with different cnt_{thresh}. Using lower cnt_{thresh} allows config change to be more adaptive to the environmental changes. However, it can also reduce the average LQ of the link due to LQ fluctuations.

Table 10
Distribution of LQ for all measurements across all links, radio configurations, and time in different testbeds. UWB links exhibit a pattern similar to other low-power radios, with the majority of links falling into the good or bad region.

Testbed	Link quality		
	Good	Intermediate	Bad
Hallway	0.42	0.1	0.48
Bridge	0.44	0.09	0.47
CLOVES	0.47	0.15	0.38
Office	0.36	0.18	0.46

7.1. Link quality distribution

As discussed in Section 2, wireless links exhibit a wide range of LQs. Previous studies have highlighted that LQ distribution varies among radio technologies. Specifically, low-power radios show a higher proportion of good and bad LQ [5]. In contrast, high-power radios often have a greater volume of intermediate LQs [3]. This understanding of LQ distribution can be valuable for network designers when selecting appropriate network routing protocols.

Table 10 provides an overview of the distribution of LQ across time, space, and different radio configurations in all testbeds. The results demonstrate that UWB links are predominantly good ($LQ > 0.9$) or bad ($LQ < 0.1$). We observed that approximately 75% of intermediate links in the CLOVES testbed and 80% of these intermediate links in the office testbed belonged to radio configurations 1 to 5 in Table 9. With DW recommended configurations (CONF ID 0 and 6), links have minimum or maximum robustness, exhibiting binary behavior compared to the intermediate radio configurations that partially increase the robustness.

7.2. Temporal effects and link stability in UWB

To measure the stability of the links with different radio configurations throughout the long-run experiment, we collected all LQ measurements and grouped them based on the link and radio configuration. Then, we calculated the average ($\overline{LQ}$) and standard deviation ($\sigma(LQ)$) of LQ for each group. Fig. 14 illustrates the LQ time series for two links. The LQ for the link with $\sigma(LQ) = 0.07$ was stable throughout the long-run experiment, while the link with $\sigma(LQ) = 0.24$ had LQ fluctuations, demonstrating a bursty behavior.

With $\sigma(LQ)$ representing LQ stability, Fig. 15 illustrates the cumulative distribution function (CDF) of $\sigma(LQ)$ for all groups. According to this figure, in both the office and the CLOVES testbeds, 75% of the links had $\sigma(LQ) < 0.1$, indicating a stable behavior.

Fig. 16 illustrates the correlation between $\overline{LQ}$ and $\sigma(LQ)$. It reveals that around 80% of the links with $LQ > 0.9$ in the CLOVES and office testbeds had $\sigma(LQ) < 0.1$. This finding suggests that $LQ > 0.9$ not only corresponds to better performance but also enhances link stability.

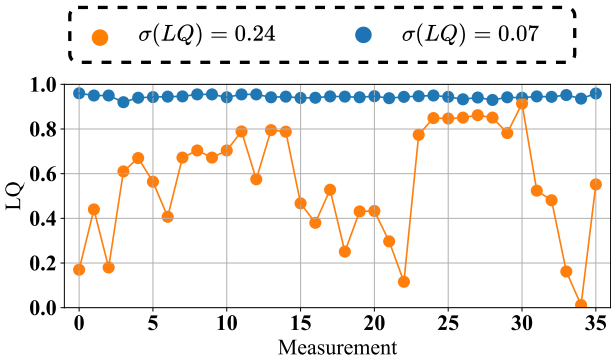

Fig. 14. LQ measurements of a bursty ($\sigma(LQ) = 0.24$) and a stable ($\sigma(LQ) = 0.07$) link in our long-run experiment. The stable link maintained the average LQ throughout the four days of data collection while the bursty link experienced LQ fluctuations.

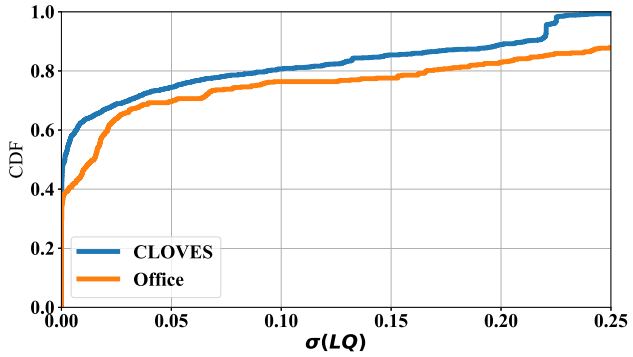

Fig. 15. The CDF of $\sigma(LQ)$ in the long-run experiment. More than 75% of the LQ measurements had $\sigma(LQ) < 0.1$ in the office and the CLOVES testbeds, indicating a stable behavior over the long-run experiment.

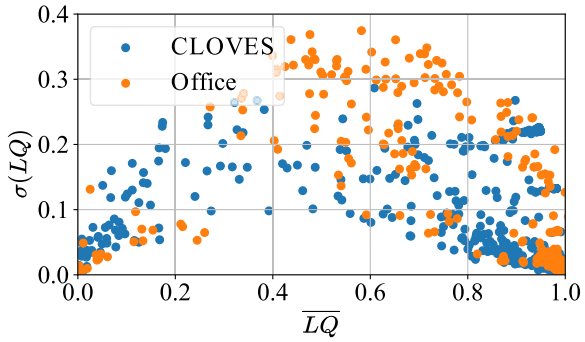

Fig. 16. Average LQ of the links and their standard deviation. Links with good or bad LQ were mostly stable in the long-run experiment.

7.3. Link quality asymmetry in UWB network

Link quality asymmetry in wireless links focuses on the LQ difference at the two ends of a two-way link. Understanding this topic guides researchers in incorporating different methods in their design, such as using acknowledgment messages. We calculated the LQ difference for both ends of each link. Fig. 17 demonstrates the CDF of LQ asymmetry in the CLOVES and the office testbed. According to this figure, almost 90% of the links had less than 0.1 LQ difference, indicating a symmetric link.

Similar to the link stability analysis, Fig. 18 shows the correlation between the LQ difference and the $\overline{LQ}$. The red line in the plot illustrates the maximum LQ difference associated with the $\overline{LQ}$. This plot illustrates that links with intermediate $\overline{LQ}$ values exhibit higher LQ

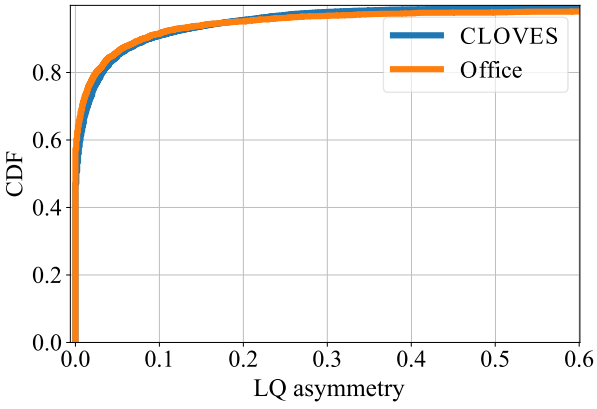

Fig. 17. CDF of standard deviation of LQs in the CLOVES testbed in the long-run experiment.

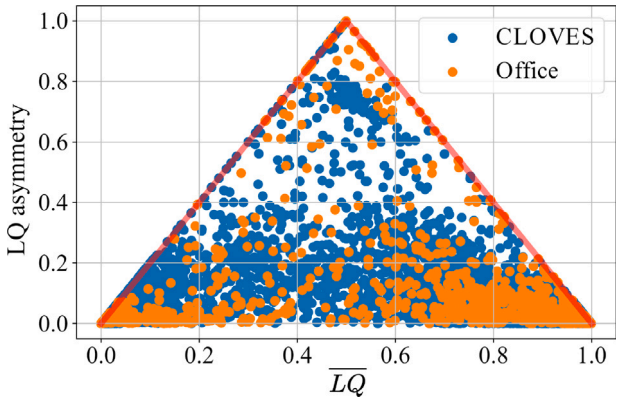

Fig. 18. Average LQ of the links and their LQ difference in the office and the CLOVES testbed. Links with good or bad LQ mostly had similar LQ in both sides of the link.

asymmetry compared to links with good or bad link quality. Furthermore, in the subset of links where one node had an LQ greater than 0.9 from the other node, our analysis revealed that in 87% of these links in the office testbed and 97% of these links in the CLOVES testbed, the other node also had an LQ greater than 0.9. This finding highlights the LQ symmetry observed when both nodes have good reception quality.

8. Conclusion

In this work, we studied and evaluated the behavior of UWB links from two different perspectives. We first evaluated the effect of UWB PHY layer parameters by observing the behavior of the link in real-world implemented testbeds and measured the amount of link quality enhancement gained when switching each parameter. Based on these findings, we redefined some of the DW recommendations and developed our config change method that provides the same LQ while reducing the trade of energy consumption and transmission time. We also studied the characteristics of the UWB links in our office testbed. The results of our study can be useful as guidelines for improving communication performance in UWB networks with static or adaptive PHY layers.

CRediT authorship contribution statement

Alireza Ansaripour: Conceptualization, Data curation, Formal analysis, Methodology, Resources, Software, Supervision, Validation, Visualization, Writing – original draft, Writing – review & editing. **Milad Heydariaan:** Conceptualization, Formal analysis, Methodology,

Resources, Validation. **Omprakash Gnawali:** Data curation, Formal analysis, Resources, Supervision, Validation, Visualization, Writing – original draft, Writing – review & editing.

Declaration of competing interest

The authors declare that they have no known competing financial interests or personal relationships that could have appeared to influence the work reported in this paper.

Data availability

Data will be made available on request.

References

[1] H. Mohammadmoradi, M. Heydariaan, O. Gnawali, SRAC: Simultaneous ranging and communication in UWB networks, DCOSS, 2019, pp. 9–16.

[2] J.F. Schmidt, D. Neuhold, J. Klaue, D. Schupke, C. Bettstetter, Experimental study of UWB connectivity in industrial environments, in: 24th European Wireless Conference, 2018, 2018, pp. 1–4.

[3] B.A. Chambers, The Grid Roofnet: A Rooftop Ad Hoc Wireless Network (Ph.D. thesis), Massachusetts Institute of Technology, 2002.

[4] N. Baccour, A. Koubâa, L. Mottola, M.A. Zúñiga, H. Youssef, C.A. Boano, M. Alves, Radio link quality estimation in wireless sensor networks: A survey, ACM Trans. Sens. Netw. 8 (4) (2012).

[5] L. Mottola, G.P. Picco, M. Ceriotti, Ş. Gunundefined, A.L. Murphy, Not all wireless sensor networks are created equal: A comparative study on tunnels, ACM Trans. Sens. Netw. 7 (2) (2010).

[6] K. Srinivasan, P. Dutta, A. Tavakoli, P. Levis, An empirical study of low-power wireless, ACM Trans. Sensor Netw. 6 (2) (2010) 1–49.

[7] M. Stocker, H. Brunner, M. Schuh, C.A. Boano, K. Römer, On the performance of IEEE 802.15. 4z-compliant ultra-wideband devices.

[8] B. Großwindhager, C. Alberto Boano, M. Rath, K. Römer, Enabling runtime adaptation of physical layer settings for dependable UWB communications, WoWMoM, 2018, pp. 01–11.

[9] DW1000 datasheet, 2021, https://www.decawave.com/sites/default/files/resources/dw1000-datasheet-v2.09.pdf. [accessed 27-Jan-2021].

[10] DW1000 user manual, 2023, https://www.qorvo.com/products/d/da007967. [accessed 13-May-2023].

[11] N. Reijers, G. Halkes, K. Langendoen, Link layer measurements in sensor networks, in: IEEE MASS, 2004, 2004, pp. 224–234.

[12] G. Holland, N. Vaidya, P. Bahl, A rate-adaptive MAC protocol for multi-hop wireless networks, in: MobiCom, 2001.

[13] A. Kamerman, L. Monteban, WaveLAN®-II: A high-performance wireless LAN for the unlicensed band, Bell Labs Tech. J. 2 (3) (1997) 118–133.

[14] B.j. Lee, S. hwan Lee, S.h. Rhee, Rate-adaptive MAC protocol for efficient use of channel resource in wireless multi-hop networks, in: ICUFN, 2010, pp. 115–120.

[15] Y. Xi, B.-s. Kim, J.-b. Wei, Q.-y. Huang, Adaptive multirate auto rate fallback protocol for IEEE 802.11 WLANS, in: MILCOM 2006 - 2006 IEEE Military Communications Conference, 2006, pp. 1–7.

[16] M. Bor, U. Roedig, LoRa transmission parameter selection, DCOSS, IEEE, 2017, pp. 27–34.

[17] M. Heydariaan, S. Yin, O. Gnawali, D. Puccinelli, D. Giustiniano, Embedded visible light communication: Link measurements and interpretation, EWSN '16, 2016.

[18] K. Gururaj, A.K. Rajendra, Y. Song, C.L. Law, G. Cai, Real-time identification of NLOS range measurements for enhanced UWB localization, in: 2017 International Conference on Indoor Positioning and Indoor Navigation, IPIN, 2017, pp. 1–7.

[19] Z. Zeng, S. Liu, L. Wang, NLOS identification for UWB based on channel impulse response, in: 2018 12th International Conference on Signal Processing and Communication Systems, ICSPCS, 2018, pp. 1–6.

[20] IEEE, IEEE standard 802.15. 4-2015 (Revision of IEEE std 802.15. 4-2011), 2016.

[21] D. Molteni, G.P. Picco, M. Trobinger, D. Vecchia, Cloves: A large-scale ultra-wideband testbed, SenSys '22, Association for Computing Machinery, 2023, pp. 808–809.

[22] RadinoL4, 2021, https://wiki.in-circuit.de/index.php5?title=radinoL4_DW1000. [accessed 12-Nov-2021].

[23] EVK1000, 2023, https://www.qorvo.com/products/p/EVK1000. [accessed 13-May-2023].

[24] K. Gururaj, A.K. Rajendra, Y. Song, C.L. Law, G. Cai, Real-time identification of NLOS range measurements for enhanced UWB localization, in: 2017 International Conference on Indoor Positioning and Indoor Navigation, IPIN, 2017, pp. 1–7.

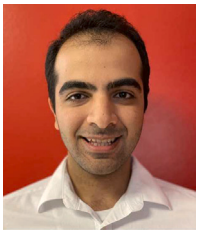

Alireza Ansaripour is a doctorate student majoring in Computer science at the University of Houston. He received his master's degree in computer networks at the Amirkabir University of Technology and his bachelor's degree at the Sharif University of technology. His research interests are wireless networks, indoor positioning and localization, and ultra-wideband radios.

Milad Heydariaan obtained his Ph.D. degree from University of Houston in 2020 and his bachelor's degree from Sharif University of Technology in 2014. His research interests are wireless networks, indoor positioning and localization, ultra-wideband radios.

Omprakash Gnawali is an Associate Professor at the University of Houston, USA. He was a Postdoctoral Scholar at Stanford University, got his Ph.D. from the University of Southern California, and received his Masters and Bachelors degrees from the Massachusetts Institute of Technology. His research lies at the intersection of wireless networks, sensing systems, and Internet technologies.